

UCLA

UCLA Electronic Theses and Dissertations

Title

Quantitative Evaluation Criteria for the Mechanical Properties of Orthodontic Clear Aligners

Permalink

<https://escholarship.org/uc/item/1x11r1r8>

Author

Nguyen, Alan Tri

Publication Date

2020

Peer reviewed|Thesis/dissertation

UNIVERSITY OF CALIFORNIA

Los Angeles

Quantitative Evaluation Criteria for the Mechanical Properties of Orthodontic Clear Aligners

A thesis submitted in partial satisfaction of the
requirements for the degree of Master of Science
in Oral Biology

by

Alan Tri Nguyen

2020

© Copyright by

Alan Tri Nguyen

2020

ABSTRACT OF THE THESIS

Quantitative Evaluation Criteria for the Mechanical Properties of Orthodontic Clear Aligners

by

Alan Tri Nguyen

Master of Science in Oral Biology

University of California, Los Angeles, 2020

Professor Kang Ting, Co-Chair

Professor Benjamin Wu, Co-Chair

Orthodontic clear aligners as an alternative to traditional braces have become increasingly ubiquitous in the last decade, thanks in part due to more cost-effective manufacturing and material advances. Combined with the recent expiration of numerous clear aligner design and manufacturing patents in 2017, there has since been an increase in new aligner varieties entering the market. With this trend comes new challenges, one of which is benchmarking their relative performance, as pre-established and standardized measures do not yet exist. The current literature on orthodontic clear aligners has, to date, a strong focus on qualitative properties such as optical clarity, stain resistance, and patient comfort levels to name a few. Of the studies that do pertain to mechanical properties, however, the intrinsic mechanical properties of the aligners are not the central focus. Moreover, the effects of the intra-oral environment such as temperature and moisture have often been overlooked.

In the current study, our main objective is to establish a novel set of testing parameters for orthodontic clear aligners by applying testing methods from the fields of material science and mechanical engineering. The mechanical tests include 1) microhardness (n=6), 2) crack-resistance (n=3), 3) stress-strain (n=6), and 4) stress-relaxation (n=3). Two different aligner materials were chosen to represent the current available selection on the market, namely polyethylene terephthalate (PETG) and thermoplastic urethane (TPU). We hypothesize that our testing methods will be able to adequately distinguish between 1) the two selected material types, 2) varying material thickness (0.625mm vs 0.750mm), 3) heat treatment via thermoforming, and 3) exposure to simulated intra-oral conditions (temperature and humidity). Lastly, the resulting modulus from the stress-strain testing will be used as an input parameter for establishing an aligner mesh model for biomechanical simulation using the finite element method (FEM).

The selected mechanical testing methodologies have proven to be valuable in distinguishing between aligner material type, thickness, status of heat treatment, and soaking. With microhardness testing, both differences in heat formation and material selection could be detected, but it is best applied in the Dry state. For crack or impact resistance testing, the ability to distinguish between material types was not a difficult task, although it had issues with thickness differences and soaked samples. With stress-strain testing, distinguishing between materials was not an issue either in the Dry state at 0.625mm. Furthermore, it is promising since for TPU in all conditions it could distinguish for soaked and thickness status. Similarly, stress-strain results indicate a faster rate of relaxation for TPU overall. Lastly, a functional finite element model was successfully developed in the current study for future use in order to better model the physical behavior of a clear aligner given assigned material properties.

The thesis of Alan Tri Nguyen is approved.

Carl A. Maida

Kang Ting, Committee Co-Chair

Benjamin Wu, Committee Co-Chair

University of California, Los Angeles

2020

TABLE OF CONTENT

ACKNOWLEDGEMENTS.....	VIII
INTRODUCTION.....	1
OBJECTIVES AND SPECIFIC AIMS.....	4
MATERIALS AND METHODS.....	5
RESULTS.....	12
DISCUSSION.....	24
CONCLUSIONS.....	27
REFERENCES.....	28

LIST OF FIGURES

Figure 1. Mechanical Retention Setup for Clear Aligners with Attachments.....	2
Figure 2. Biostar Vacuum Former.....	5
Figure 3. Vicker’s Diamond Pyramid and Calculation.....	7
Figure 4. “Dog Bone” or Dumbbell Shaped Template for Stress-strain and Stress-relaxation Testing ...	9
Figure 5. Microhardness Results for PETG and TPU	12
Figure 6. Inner versus Outer Microhardness for Aligned PETG and TPU.....	13
Figure 7. Quantile-quantile (QQ) Plot for Crack Resistance.....	14
Figure 8A-D. Impact Test Results @2kg for PETG and TPU.....	15
Figure 9A) Stress-Strain summary graph for Modulus (MPa), and B) Quantile-quantile plot for visualizing normality.....	17
Figure 10. "Necking" Phenomenon.....	17
Figure 11. Example of Stress-Strain curve for PETG 0.750mm.....	17
Figure 12A) Tensile Stress Change (MPa) after 3 hours, and B) Stress-Relaxation profile of TPU vs PETG.....	18
Figure 13. Quantile-quantile Plot for Stress-Relaxation.....	19
Figure 14. Initial Import into Materialise Mimics.....	20
Figure 15. Meshing in Materialise 3-Matics.....	20
Figure 16. Reduction of Number of Mesh Elements.....	21
Figure 17. Refined Mesh after Smoothing and Noise Removal.....	21
Figure 18. Calibration of Aligner Model Thickness.....	22
Figure 19. Finite Element Analysis Simulation on Clear Aligner Model.....	22

LIST OF TABLES

Table 1. Study Design	5
Table 2. Summary Table for Stress-Strain (MPa) Values for PETG and TPU Raw.....	17
Table 3. Summary Table for Stress-Relaxation: Tensile Stress (MPa).....	19

ACKNOWLEDGMENTS

I would like to first and foremost thank all the individuals who have helped make this project a reality, from offering their expertise to providing support and invaluable guidance along the way.

First, I would like to thank both Dr. Kang Ting and Dr. Chia Soo for giving me the unique opportunity to work in their laboratory over the past 9 years. I have been continuously challenged with new, cutting-edge projects that I have had the opportunity to share both nationally and to an audience abroad. And never would I have imagined that we would one day collaborate with NASA and SpaceX for rodent microgravity studies. These invaluable yet diverse experiences have only further amplified my curiosity as a student and clinician.

This project would also not be possible without crucial guidance from the UCLA Bioengineering team led by Dr. Benjamin Wu. His unique expertise and insight in all matters related to material science, bioengineering, and prosthodontics have been nothing short of invaluable for this project. I am also incredibly grateful to work under Dr. Yulong Zhang as my mentor, helped contribute towards the project design and testing methodologies. The aligner thickness measurements would also not be possible without my colleague, Dr. Fangming Li.

In addition to Dr. Kang Ting and Dr. Benjamin Wu, I would like to thank Dr. Carl Maida for agreeing to serve on my committee and providing me with a more holistic context for my research. Special thanks to Dr. Won Moon and Dr. JinHee Kwak for their clinical aligner expertise and early project design guidance. Lastly, this thesis would not be possible without the guidance and support from Dr. Haofu Lee, Dr. Xinli Zhang, and Mr. Matthew Dingman.

INTRODUCTION

Clear aligners have played an integral role in changing the landscape of modern orthodontic treatment^{1,2}. As the name implies, they are used to align teeth usually in lieu of, if not in conjunction with, traditional fixed appliances or braces while prioritizing esthetics in the process. With advancements in technology driving down the cost of 3-dimensional printing and manufacturing, paired with the recent 2017 expirations of numerous key Invisalign (Align Technology™) patents, the influx of new aligner varieties entering the market is rapidly increasing^{2,3}. However, as will be discussed, the current literature does not yet provide clear, objective standards by which these clear aligners can be evaluated for their intrinsic mechanical properties. Without such a basis for comparison, it will prove increasingly difficult to verify and distinguish between the claimed efficacies for new aligner products. As such, it is now more important than ever to establish a viable set of mechanical evaluation criteria to compare orthodontic clear aligners.

Although subtle compositional differences exist between aligners, all aligners as polymers are subject to intraoral forces and will thus experience some degree of material wear. The majority of current aligner material compositions are variations of polyurethane resin, a polyethylene copolymer, or polypropylene copolymer^{4,5}. Invisalign®, perhaps the most well-known, is speculated to consist of layered polyurethane methylene diphenyl diisocyanate and 1,6-hexanol with additives⁵. In light of any significant compositional differences, however, Elisades *et. al.* had wisely noted in 1999 that essentially all “aligner materials are resin polymers, which, not being inert, are subject to changes in the warmth, humidity, mastication forces and prolonged contact with salivary enzymes in the oral environment”⁶. This suggests that many factors are indeed at play, and thus provide us with a general guideline for the current study in which we must curate the appropriate mechanical tests. To date, only a handful of studies have briefly evaluated the intrinsic material properties of the clear aligner material themselves. Even fewer have attempted to account for the intraoral environment (temperature and moisture) on the mechanical properties of clear aligners, as Elisades *et. al.* had alluded to⁶.

In the current literature, the overwhelming majority of studies pertain to qualitative features, such as optical clarity, stain resistance, and patient discomfort levels with impact strength being the extent of the biomechanical discussion ⁶⁻⁸. While there are several quantitative studies on the effects of aligners on tooth movement ⁹, they often ignore the physical, intrinsic properties of the aligner material themselves. For instance, a study by Drake *et. al.* in 2012 had set out to evaluate aligner fatigue, but does so by analyzing its effect on decreased orthodontic tooth movement ⁹. However, this is not to discredit the importance of these types of studies. Nevertheless, many investigators like Elisades *et al.* will agree that the next step is to evaluate this biomechanical question, especially in the intra-oral environment ^{6, 10-12}.

Of the existing literature, there are in total only two main studies outside of our group that have focused on analyzing aligner properties. The first was in 2015, by Alexandropoulos *et. al.* which compared four commercially available aligners and tested for a variety of parameters, including Marten's hardness, indentation modulus, elastic to total work ratio, indentation creep ⁵. The second group, Lombardo *et. al.* (2017), also compared four aligners but for their yield strength and stress-relaxation in a 24-hour *in vitro* study ⁴. While this focused on key material property tests, it is also one of the first studies in the aligner field to control for temperature as well as moisture. This study had also concluded that aligners are strongly influenced by their materials of construction, and that stress release change at least under 24 hours of orthodontic loading ⁴.

In summary, the limitations of the current literature provide a strong rationale for the current study. Besides the mechanical studies mentioned above, there are no other studies that directly evaluate the intrinsic mechanical properties of clear aligners, despite numerous early studies pointing in this direction ^{10,11}. Along these lines, there has only been one attempt to simulate the intra-oral environment ⁴. Our laboratory, in collaboration with the UCLA Section of Orthodontics and UCLA Department of Bioengineering, is adequately equipped for this undertaking. Our laboratory was one of the first to independently quantify Invisalign's distortion rate in 2002, and later for attachment efficacy in



Figure 1. Mechanical Retention Setup for Clear Aligners with Attachments. Image borrowed with permission from Kwak *et. al.*, 2015

2015 with Kwak et. al. (**Fig. 1**)^{13, 17}. And although finite element analysis (FEA) is quickly emerging as a modern biomechanical simulation tool in other fields¹⁴, only two groups have explored its potential in optimizing aligner design^{15,16}, while our lab has developed a published protocol for similar applications. Taken together, there is a clear need to establish an objective, mechanical evaluation criteria for clear aligners. Secondly, these measurements must extend to intra-oral conditions as that will have the most clinical relevance. Lastly, the latest gold standard of computer biomechanical analysis will provide more versatility in future aligner design.

Objectives & Specific Aims

As discussed earlier, the current literature is abundant with qualitative tests, such as those evaluating optical properties, stain resistance, and patient comfort levels. While these measurements are without a doubt highly valuable in the clinical setting, there is an evident void when it comes to the actual material properties of the clear aligners themselves, both before and after thermoforming. The main objective of our study, then, is to establish a novel set of testing parameters for orthodontic clear aligners by applying testing methods from the fields of material science and mechanical engineering.

AIM 1: To establish quantitative evaluation criteria for the mechanical properties of clear aligners

- a. Testing methods will include microhardness, crack (or impact) resistance, stress-strain, and stress-relaxation measurements.

AIM 2: To evaluate the effect of simulated intra-oral conditions, thickness, and thermoforming on the mechanical properties of clear aligners

- a. The aforementioned mechanical tests, where possible, will also be performed with samples subject to simulated intraoral conditions (maintained at 37.0°C and soaked in phosphate-buffered saline (PBS) soaking solution), samples of two different thicknesses (0.625mm and 0.750mm), and thermoforming.

AIM 3: To develop a refined, computer-generated finite element analysis (FEA) aligner mesh model as a platform for future virtual biomechanical testing

- a. The obtained modulus and thickness will be used as input parameters in developing a refined aligner mesh model for biomechanical simulation

MATERIALS AND METHODS

The two aligner materials that were selected for this study are polyethylene terephthalate (PETG) and thermoplastic urethane (TPU). These materials were chosen due to their ubiquitous use in orthodontic practices for clear aligner orthodontic treatment, and are representative of the materials commonly seen in many of the brand-name manufacturers. For the PETG and TPU material, both of the commercially offered thicknesses of 0.625mm and 0.750mm were chosen to represent the selection available on the market ⁵. For instance, the Essix ACE® Plastic which is commonly used measures approximately 0.750mm in thickness ^{2,17,18}.



Figure 2. Biostar vacuum former used for heat application and vacuum formation of heat-treated aligners.

In this study, the two main treatments will involve heat application and/or soaking to simulate the intra-oral environment. For the purposes of this study, the initial clear aligner material will be henceforth identified as the ‘raw’ material. By contrast, an ‘aligned’ material will indicate that the clear aligner has undergone thermoforming, or heat application followed by vacuum forming, via the protocol mentioned below. Finally, ‘soaking’ will indicate whether the clear aligner material, independent of whether it has been heat-treated or not, has been soaked in a simulated saliva solution consisting of phosphate buffered saline (PBS) for 24 hours at 37°C maintained by an incubator ¹⁹⁻²¹. Taken together, there will be in total four different treatment groups amongst the two different aligner materials with two different thicknesses.

PETG 0.625mm & 0.75mm			TPU 0.625mm & 0.75mm		
	Raw (non-heat- formed)	Aligned (Heat-formed)		Raw (non-heat- formed)	Aligned (Heat-formed)
Dry	Raw / Dry	Aligned / Dry	Dry	Raw / Dry	Aligned / Dry
Soaked (PBS 24hrs @37C)	Raw / Soaked	Aligned / Soaked	Soaked (PBS 24hrs @37C)	Raw / Soaked	Aligned / Soaked

Table 1. Study Design. Raw refers to the original untreated material, and aligned indicates after heat-treatment. Soaking indicates treatment via soaking in PBS for 24hrs at 37C in an incubator, otherwise denoted as dry.

Specifically, the process of thermoforming will utilize the Biostar Scan vacuum former (Great Lakes Dental Technologies, New York), which is commonly used in orthodontic offices for fabricating clear aligners and retainers (see **Fig. 3**). The circular ‘raw’ clear aligner disc is first secured in the ring-locking template. The thickness of the aligner is then selected via the graphic user interface of the machine. Afterwards, the heating element brings the aligner temperature to approximately 160°C, after which the locking ring is transferred and pressed down onto the model, thus activating the vacuum line. A cooling period of 45 seconds is required before the vacuum-formed aligner can be removed¹². The sample is then prepared according to the specific testing protocols discussed below.

Microhardness Testing

The microhardness test was originally developed for metal and ceramic materials, and is itself a scaled down version of the Vicker’s hardness test which utilizes an indenter. It has since been adapted to analyze composite and polymer materials, but it has seen very limited applications in orthodontic clear aligners. Typically, microhardness testing refers to the static indentations of loads less than 1 kgf. The indenter is usually the Vickers diamond pyramid, and the procedure is similar to that of a standard Vickers hardness test except that it is performed on a microscopic scale to achieve higher precision^{22,23}.

To obtain measurements for microhardness for our study, the aligner sample is cut into a 20.0 x 10.0mm rectangle and cleaned with Kimwipes®^{22,24}. Adhesive film is removed from the surface of the aligner material if present, and the sample is fixed to a glass slide via scotch tape. The specimen is then secured to the testing stage of the microhardness machine (Phase II+ 900-392B Micro Vickers Hardness Tester, Phase II Plus Instruments, New Jersey, USA). The load is then set to 200gf with a dwell time of 15 seconds. The height is then adjusted at the 40x objective in order to clearly visualize the specimen. After achieving focus, the objective lens is switched to the diamond indenter, ensuring that the test surface is perpendicular to the diamond indenter, and the load is applied. If the sample was moved during the testing, the testing was repeated.

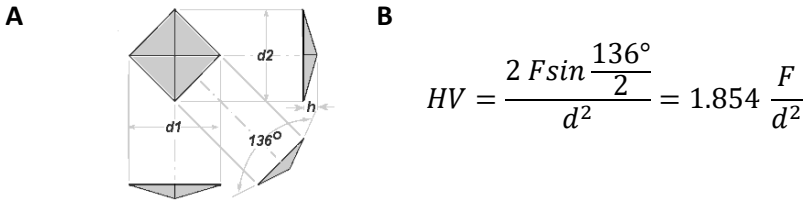


Figure 3. Vicker's Diamond Pyramid and Calculation. A) Vickers diamond pyramid is shown with an angle of 136° between faces, with d_1 and d_2 representing the diagonal distances in the horizontal and vertical position, respectively. B) Vickers hardness (HV) is a function of the load in kgf (F), as well the mean of the two diagonals d_1 and d_2 , or d .

The indenter is then rotated back to the 40x objective, and the left filar line is adjusted such that the inner edge of the line touches the left most point of the cross-impression²². The right side of the line is brought to coincide with the left line, and the value is zeroed after which the right line is brought to the right-most point of the cross-impression to obtain the first diagonal measurement (d_1). The eyepiece is then rotated to the orthogonal position and the filar line adjusted to obtain the second diagonal measurement (d_2) (**Fig. 3A**). The diagonal length is entered, and the Hardness value is subsequently calculated, which itself is a function of the load (F) and the mean of the two diagonals (d) (**Fig. 3B**).

Although there is now an increasing trend of reporting the Vickers hardness in SI units (ie MPa or GPa), the value is normally expressed as a dimensionless integer, without the units kgf/mm^2 . Furthermore, in our preliminary tests, three different loads, specifically 100, 200, and 300 gf²³, were used to determine the ideal load for testing a various aligner materials. Ultimately, our group had isolated the 200gf as the most suitable load to distinguish between different materials and treatment conditions.

Crack Resistance Testing

Crack resistance testing, also referred to as impact testing, is commonly used in the industry to test the impact resistance of various coatings and materials^{25,26}. These include plastic sheets and molded plastics, and examination involves visual inspection for signs of failure that include cracking or puncture. Common testing protocols have been established where the methods and parameters have been defined, of which include ASTM D2794, ASTM G-14, and ASTM D-4226²⁷. These require only minor modifications to adapt to the Gardner Impact Tester used in this study (PF-5545 Gardner Heavy-Duty Impact Tester, BYK Additives & Instruments, Wesel, Germany), utilizing either a 1kg or 2kg weight²⁶.

The circular aligner disc is placed on the anvil at the target point, with the punch in the punch holder. The round-nosed punch tip measures 1.59cm in diameter, with the inner ring diameter of the complementary die at 1.63cm. The vertical position of the lifting screw is readjusted to the zero mark, accounting for the specimen thickness in order to calibrate the instrument. The weight (either 1kg or 2kg) is then loaded into the tube, raised to the desired height as indicated by the lifting screw and then released ²⁶. The specimen is then removed and evaluated. In measuring the impact, the units are that of energy, specifically the kinetic energy at the instant of impact from the falling weight. This is also equivalent to the energy required to lift the weight to the initial height, as well as the potential energy at the moment the weight is released ²⁶. We assume here that the friction from the weight against the tube is negligible, such that any energy loss attributed to friction is then non-existent. Lastly, since the potential energy is the product of the weight multiplied by the height of weight release, the guide tube uses a linear scale.

Impact testing allows us to determine the amount of energy required to achieve failure of a specimen type. In the context of this study, impact testing provides a standard for impact resistance and a benchmark for which to compare to other materials. The criteria for failure can be arbitrarily established by the user, and in this study we have defined it as a puncture encompassing at least 180°, or a half circle. The height of the puncture was also measured in millimeters to establish a linear relationship leading up to failure.

Stress-Strain Testing

For the stress-strain test, the specimen is cut into a specific “dog bone” or dumbbell-shaped that is designed to be fixed at the two ends and ensure that deformation or breakage occurs in the middle region of the specimen ^{28,29}. The sample should be 90.0mm in length, and 22.0mm wide at the ends, but 6.0mm wide at the narrowest section for the middle region as shown in the **Fig. 4** below.

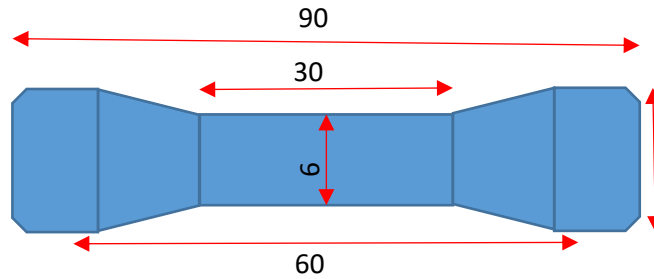


Figure 4. “Dog Bone” or dumbbell shaped template for stress-strain and stress-relaxation testing. Measurements in mm.

The universal testing machine (Instron 5500 Standard Compression Tension Tensile Universal Testing Machine, Instron, Massachusetts, USA) is then powered on, and the two clamps are applied at a distance of 60.0mm apart when fixing the specimen in place. The Bluehill software is then used to test, with the stress-strain set to have a ramp rate of 5 mm/min, and a stop condition of 5.0 mm of extension if not manually stopped after significant yielding is observed ²⁸. Once the measurement is completed, the stress-strain profile data output is saved.

Stress-relaxation Testing

For the stress-relaxation test, the specimen was prepared using the same method as for the stress-strain testing. The specimen is then fixed onto the Instron machine clamp, and the Bluehill® Universal Test software (Instron, Massachusetts, USA) is used to obtain the measurements. The stress-relaxation method is chosen, with the testing conditions set to a constant ramp rate of 5.0mm/min, and the hold value set to a threshold of 36.0 MPa (or approximately 50% of the predicted yielding stress) ³⁰. Each sample is held for a continuous 16 hours before the final measurement is obtained and the profile data saved.

Finite element analysis

Computer tomography (CT) of the human dentition will be acquired from the online data base in the form of a Digital Imaging and Communication in Medicine (DICOM) file. This volumetric data will then be imported into the Materialise Mimics software (version 13.1, Materialise, Leuven, Belgium). The volumetric

data will be applied a threshold segmentation range of 238-3071 Hounsfield units, which will be sufficient to capture the hard tissue of interest (enamel of dentition) ³⁴. The model will be cleaned for any noise, and segmented for the volume of interest ³⁴. Subsequently, the converted three-dimensional model will be imported into Materialise 3-matics (version 9.0, Materialise, Leuven, Belgium), where the model will be converted into a mesh. The mesh will manually be modified to further reduce noise, and Laplacian function is applied as a smoothing filter. Triangle reduction is applied to remove any overlapping, redundant triangles. The 3D object will finally be re-meshed to reduce and optimize the number of elements and nodes to simplify the calculation for finite element analysis. The finalized meshed model is then converted from TET(4) into TET(10) elements to further improve accuracy in calculating the finite element model, and exported as an .INP model file ³⁴.

To create the aligner material from the three-dimensional model of the dentition, an inverse shell function will be used to complement the surface morphology, or essentially create a negative mold that is the aligner, in the Materialise 3-matics software. Thicknesses of the material will then be calibrated using actual measurements. Further, the specific material properties will be based on our measured Young's modulus, with Poisson's ratio for polyurethane derived from the literature. This aligner model will follow the same aforementioned protocol for smoothing, noise reduction, and mesh element reduction. Our refined mesh model after processing consisted of 52,516 elements, which will be more than adequate in producing accurate simulations. The TET(4) elements will finally be converted to TET(10) elements before being exported as an .INP file for finite element analysis.

After the import of refined mesh model of the aligner into ABAQUS (version 6.12, Dassault Systèmes, France), the volumetric elements and nodes will be isolated. The material will be assumed to be homogenous and isotropic. While for the enamel the a Young's modulus of 15GPa and Poisson's ratio of 0.33 will adequately represent the dentition ³⁵, again the Young's modulus and Poisson's ratio for the aligner materials will be determined by the results of the stress-strain and dynamic mechanical analyses ³⁶. The parameter for success here will be that the finite element simulation is able to run successfully for the aligner model under applied load.

Statistical Analysis

The statistical analyses and power for this study was calculated using the GraphPad Prism v.8.4.2 with guidance from the UCLA Biostatistics Department. Normality tests were performed for data sets using both the Anderson Darling (A2) test and the Shapiro Wilk (W) test with an alpha = 0.05³⁷. Given that the data set is normal, statistical significance will then be determined using factorial level analysis of variance (ANOVA) to compare the means between different treatment groups with statistical significance set at $p < 0.05$, followed by a post-hoc analysis for more specific comparisons using Tukey's test²⁴. If the data set does not show a normal distribution, then the Kruskal-Wallis H test will be utilized.

RESULTS

Microhardness

For microhardness, the Shapiro-Wilk (W) statistical analysis at $\alpha = 0.05$ with a calculated W of 0.9059 does not exceed the 0.916 required, and the normal distribution is confirmed with the Anderson-Darling (A2) test with $AD = 0.6724$. A quantile-quantile (QQ) plot is shown below to visualize the normal distribution. In lieu of a more complex 4-way ANOVA which would increase the number of interactions and likelihood of false positives, four separate 3-way ANOVA tests were used ($n=6$).

Three-way factorial level ANOVA testing for within PETG shows overall significant difference between the Dry/Soaked and Raw/Aligned groups ($p = 0.0009$), and specifically only significance between 0.625mm Dry Raw versus Aligned ($p = 0.0319$). For comparisons within TPU, there was significance seen between Dry and Soaked for 0.625mm Raw ($p = 0.0067$), and between Dry and Soaked for 0.750mm Aligned ($p = 0.0003$). Further, for TPU 0.625mm, there was significance between Dry Raw and Aligned ($p = 0.0024$). For TPU 0.750mm Dry, there was significance between Raw and Aligned ($p = 0.0127$), as well as a difference between Dry Raw 0.0625mm versus 0.750mm ($p = 0.0046$). Lastly, significance was also seen for Dry Aligned TPU 0.625mm versus 0.750mm ($p = 0.0065$).

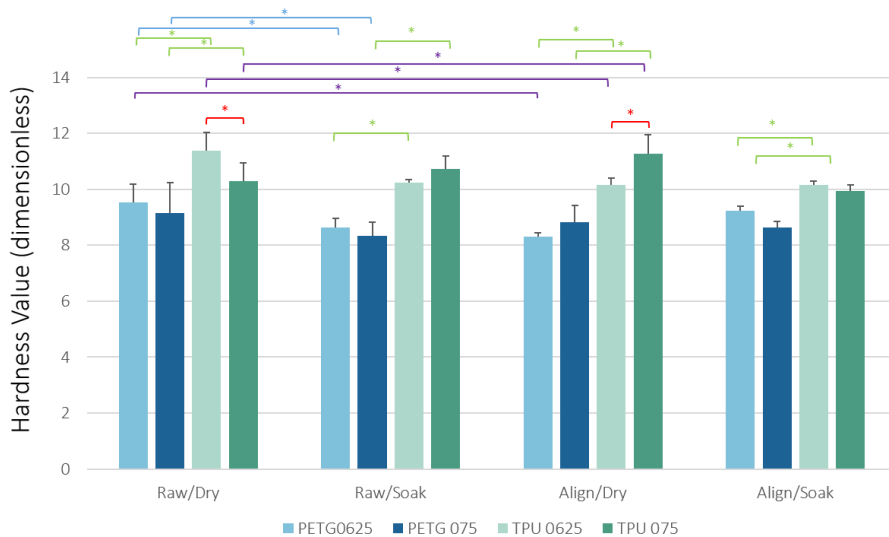


Figure 5. Microhardness Results at 200gf for PETG and TPU 0.625mm and 0.750mm. Blue significance bars illustrates differences from soaking, red for thickness, purple for heat-formation or aligning, and green for material type.

For comparisons between TPU and PETG, both at 0.750mm, we found statistical significance for Dry Raw TPU versus PETG ($p = 0.0373$). The same was also seen for Dry Aligned TPU versus PETG ($p < 0.0001$). Both Soaked Raw and Soaked Aligned between the two materials also had significant difference, with a p -value < 0.0001 and $p = 0.0022$, respectively. For comparisons between TPU and PETG at 0.625mm thickness, there was significance for the Dry Raw ($p < 0.0001$) as well as the Dry Aligned group ($p < 0.0001$) between the two materials. Further, we see a similar trend for the Soaked Raw ($p < 0.0001$) and Soaked Aligned ($p = 0.0012$) between the two materials.

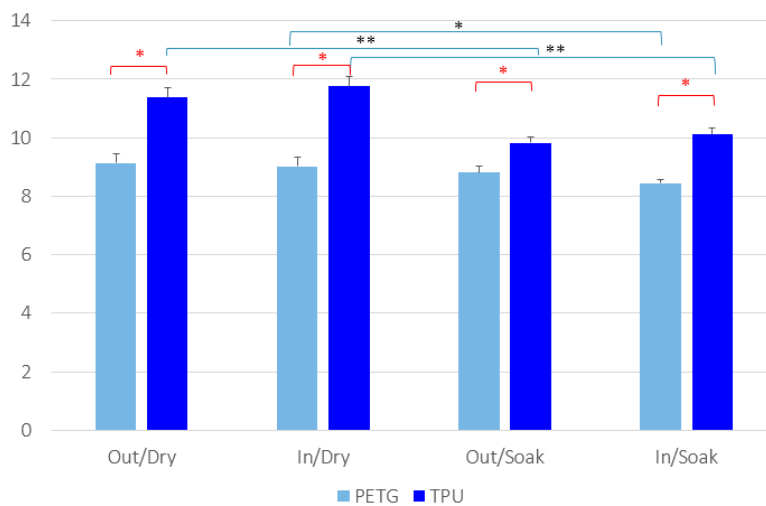


Figure 6. Inner versus Outer Microhardness for Aligned PETG and TPU 0.750mm. Red significance bars indicate significance between materials, while blue represents changes in Soaking conditions. Raw samples (not aligned) since untreated were not expected to have difference between inner and outer surfaces.

Lastly, we also tested for microhardness of the inner surface versus the outer surface for 0.750mm TPU versus PETG ($n=6$). For this test, since only the Aligned (thermoformed) samples would be suspected to have a different inner surface texture, the Raw group was discarded. The Shapiro-Wilk (W) statistical analysis at $\alpha = 0.05$ with a calculated W of 0.9770, along with the Anderson-Darling (A_2) test with $AD = 0.4040$, both confirm a normal distribution. Thus, a 3-way ANOVA analysis shows that for the same material, whether it was dry or soaked, there is no significant difference between the outer surface and inner surface for microhardness. However, there was significance between Aligned Dry and Aligned Soaked for the inner PETG surface ($p = 0.0081$). Within TPU, for both inner and outer surface there was a difference between Aligned Dry and Aligned Soaked (both $p < 0.0001$). Between the two different materials, we see that there was

significant difference for both the Aligned Dry and Aligned Soaked group, and both for inside and outside (all four with $p < 0.0001$).

Crack Resistance

For crack resistance, the Shapiro-Wilk (W) statistical analysis at $\alpha = 0.05$ with a calculated W of 0.8193 does not exceed the 0.916 required, so the distribution is not normal. This is confirmed with the Anderson-Darling (A2) test with a relatively high $AD = 4.336$, and a quantile-quantile (QQ) plot is shown below to visualize the lack of normal distribution. Since the data set fails the normal distribution assumption, ANOVA becomes invalid here and the alternative analysis, the non-parametric Kruskal Wallis H-test, was used. For PETG 0.625mm material, there was a significance between at failure between the Dry Aligned treatment compared to the Soaked Aligned. For PETG 0.750mm material, this was also the case except Dry Raw showed significant difference compared to Soaked Raw. For impact testing for TPU at 0.750mm, there was only significance between Dry Raw and Soaked Aligned, as the other treatments did not proceed to failure.

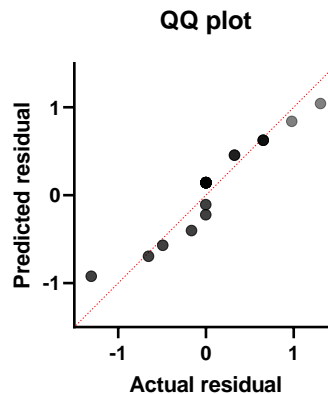
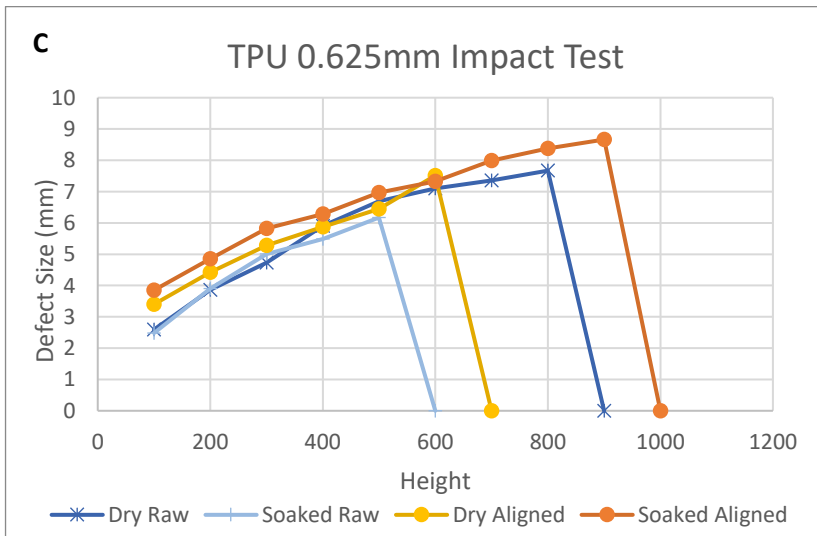
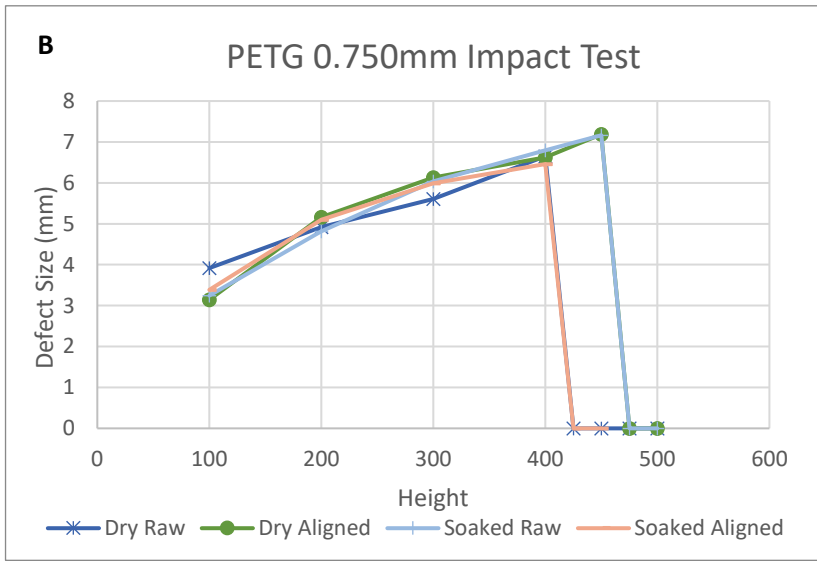
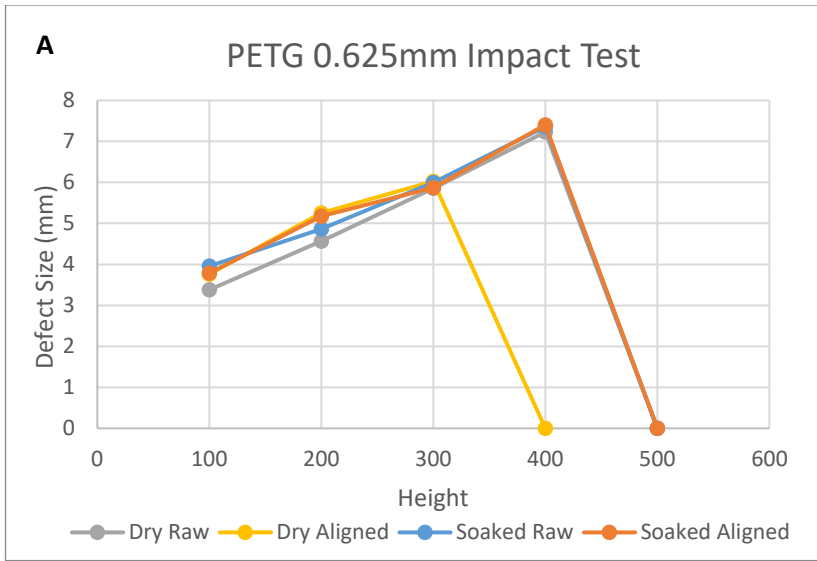


Figure 7. Quantile-quantile (QQ) Plot for Crack Resistance. Used to help visualize a normal distribution. In this case, both Anderson-Darling and Shapiro-Wilk test indicated data distribution was not normal, so ANOVA was contraindicated.



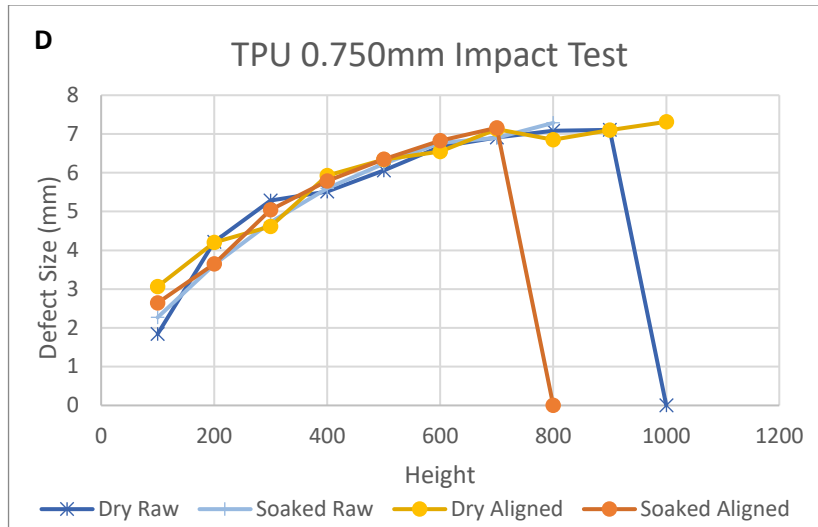


Figure 8A-D. Impact Test Results @2kg for PETG and TPU, at 0.625mm and 0.750mm. Treatment groups that proceeded to failure return to the 0 point on the Y-axis, in contrast to those that did not reach failure. Please note the difference in scale of the X-axis for PETG compared to TPU.

Stress-Strain

A three-way, factorial level ANOVA for stress-strain testing for modulus (n=6) indicated overall statistical significance for the material type ($p = 0.0034$) as well as for dryness ($p < 0.0001$). Follow-up analysis with the post-hoc Tukey's test indicates clinically relevant statistical significance between dry TPU at 0.625mm versus 0.750mm of thickness (adjusted p-value = 0.0105). For TPU 0.625mm, statistical significance was also seen for dry versus soaked (adjusted p-value < 0.0001). Finally, for TPU 0.750mm, statistical significance was also seen for dry versus soaked (adjusted p-value = 0.0438). For the dry material at 0.625mm, significance was seen between the PETG material and TPU material (adjusted p-value < 0.0001).

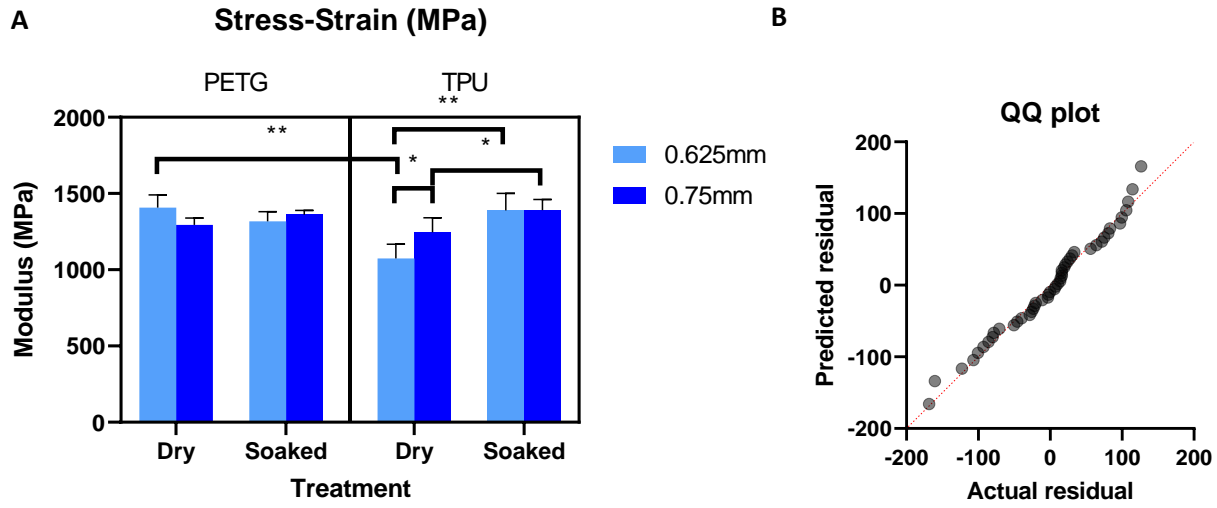


Figure 9. A) Stress-Strain summary graph for Modulus (MPa), and B) Quantile-quantile plot for visualizing normality.

	PETG (MPa)	TPU (MPa)
0.625mm Dry	1407.84 ± 82.15	1074.95 ± 92.14
0.75mm Dry	1293.83 ± 46.00	1245.372 ± 95.50
0.625mm Soak	1318.25 ± 62.17	1389.45 ± 111.84
0.75mm Soak	1361.32 ± 27.35	1391.36 ± 69.35

Table 2. Summary table for Stress-Strain (MPa) values for PETG and TPU Raw.

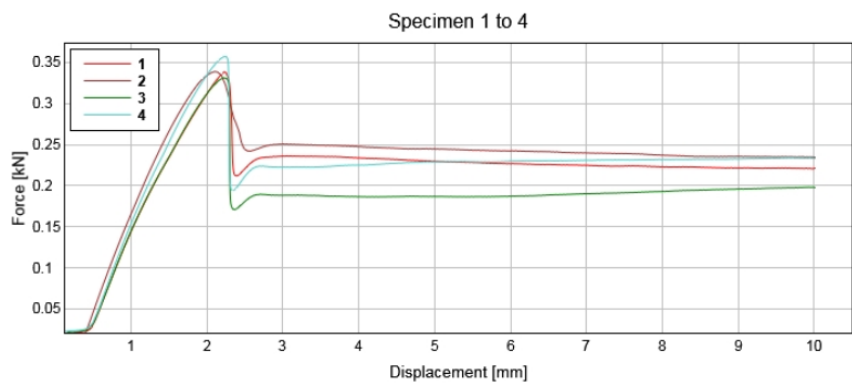


Figure 11. Example of Stress-Strain curve for PETG 0.750mm. Dry conditions are shown here up to 10mm of displacement

The Shapiro-Wilk (W) statistical analysis was performed at a threshold of $\alpha = 0.05$, and the calculated W of 0.9724 exceeds the 0.916 required to indicate a normal distribution. The Anderson-Darling

(A2) test also confirms that the data set follows a normal distribution ($AD = 0.4048$). A quantile-quantile (QQ) plot is shown below to visualize the normal distribution.

Stress-Relaxation

A two-way, factorial level ANOVA for stress-relaxation testing for change in tensile stress after an elapsed 3 hours ($n=3$) indicated overall statistical significance for the material type ($p = 0.0058$) but not for dryness ($p = 0.0971$). Follow-up analysis with the post-hoc Tukey's test indicates relevant statistical significance between the PETG and TPU material (adjusted p -value = 0.0058), with both dry and at 0.750mm thickness. Further, significance was seen between dry and soaked 0.750mm PETG (adjusted p -value = 0.0324). Lastly, a difference was calculated for dry PETG 0.750mm and soaked TPU 0.750mm in tensile stress drop-off after 3 hours (adjusted p -value = 0.0174).

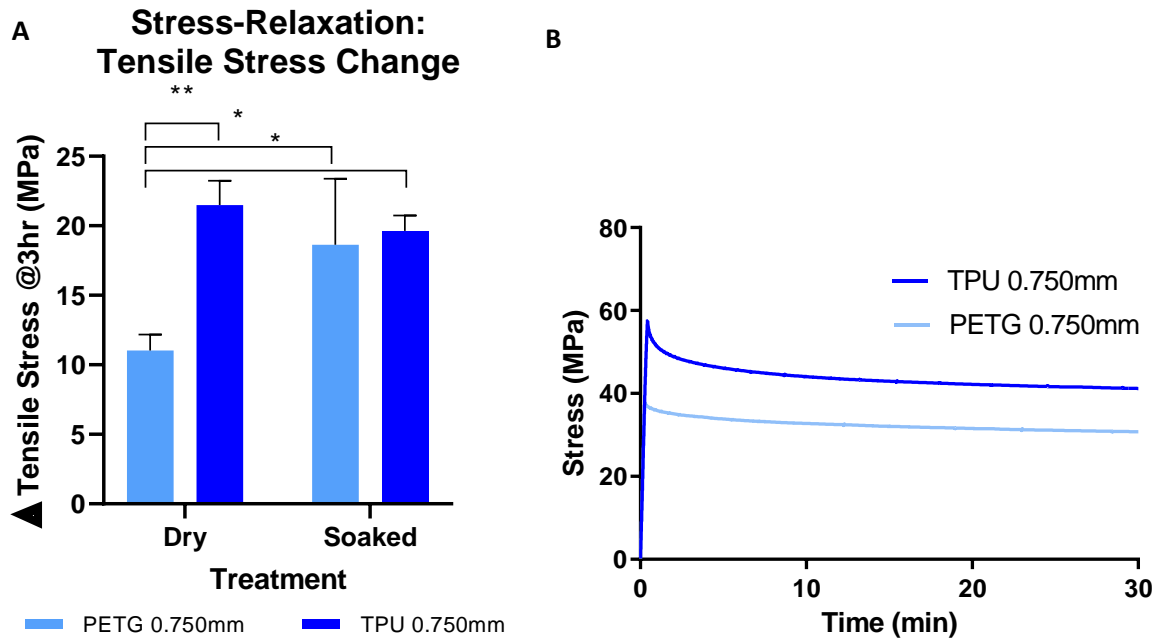


Figure 12. A) Tensile Stress Change (MPa) after 3 hours, and B) Stress-Relaxation profile of TPU vs PETG.

	Test conditions	Relaxation Rate (MPa/Hr)	Stress at t=0 hr	Stress at t=3 hr	Stress change after 3 hr
PETG	Raw, Dry	3.41	44.07 MPa	33.04 MPa	11.03 MPa
TPU	Raw, Dry	7.16	67.81 MPa	46.33 MPa	21.48 MPa
PETG	Raw, Soaked	6.21	47.51 MPa	28.86 MPa	18.64 MPa
TPU	Raw, Soaked	6.54	60.58 MPa	40.96 MPa	19.63 MPa

Table 3. Summary table for Stress-Relaxation: Tensile Stress (MPa). At t=0hr, t=3hr, and stress change after 3hrs

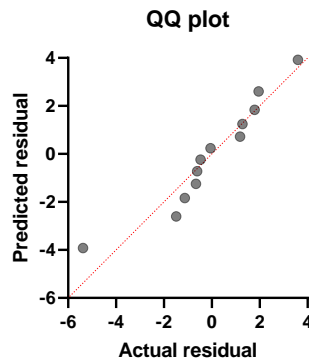


Figure 13. Quantile-quantile Plot for Stress-Relaxation.

The Shapiro-Wilk (W) statistical analysis was performed at a threshold of $\alpha = 0.05$, and the calculated W of 0.9257 exceeds the 0.916 required to indicate a normal distribution. The Anderson-Darling (A2) test also confirms that the data set follows a normal distribution ($AD = 0.4076$). A quantile-quantile (QQ) plot is shown below to visualize the normal distribution.

Finite Element Analysis

In creating the finite element analysis (FEA) model, a dental cast was first scanned using Ortho Insight 3D and saved as a .STL file. The raw volumetric import is shown below using Materialise Mimics software (version 13.1, Materialise, Leuven, Belgium). The model is then ‘cut’ to a volume of interest (VOI) that resembles the area where an aligner would cover, and the model is also cleaned for any noise at this stage ³⁴.

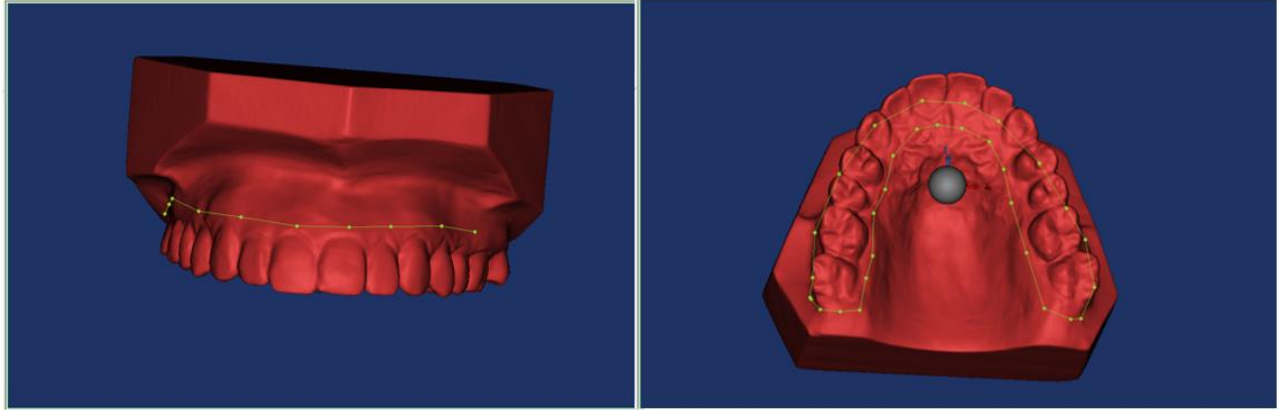


Figure 14. Initial Import into Materialise Mimics.

Subsequently, the converted three-dimensional model will be imported into Materialise 3-matics (version 9.0, Materialise, Leuven, Belgium) for mesh processing. To create the aligner model from the three-dimensional model of the dentition, an inverse shell function will be used to complement the surface morphology, or essentially create a negative mold that is the aligner, in the Materialise 3-matics software. The rough mesh is filtered to further reduce noise, and Laplacian function is applied as a smoothing filter. Triangle reduction is applied to remove any overlapping, redundant triangles. In the figure below, one can appreciate the areas of high noise and artifacts (circled in red), which will be targeted for removal.

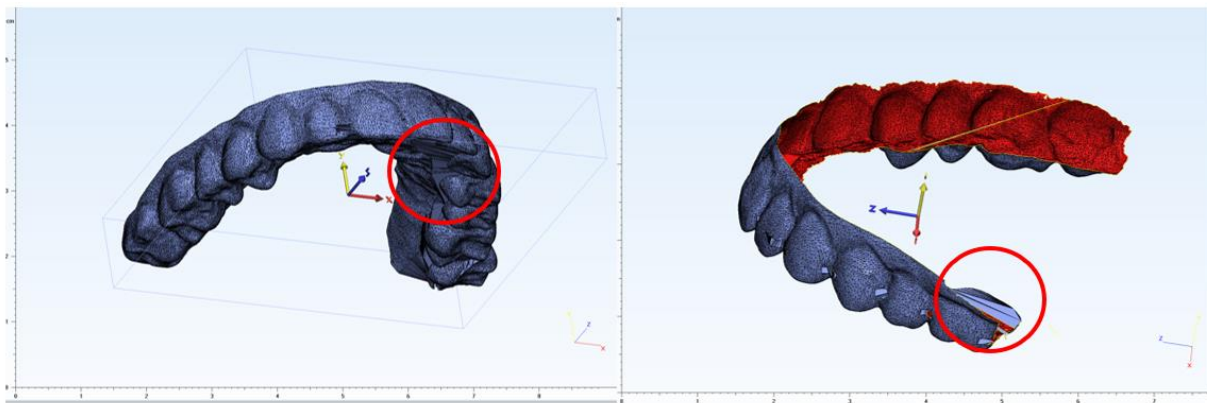


Figure 15. Meshing in Materialise 3-Matics. Unwanted artifacts are circled in red.

The 3D object will finally be re-meshed to reduce and optimize the number of elements and nodes to simplify the calculation for finite element analysis. Our refined mesh model after processing consisted of 52,516 elements, which will be more than adequate in producing accurate simulations.

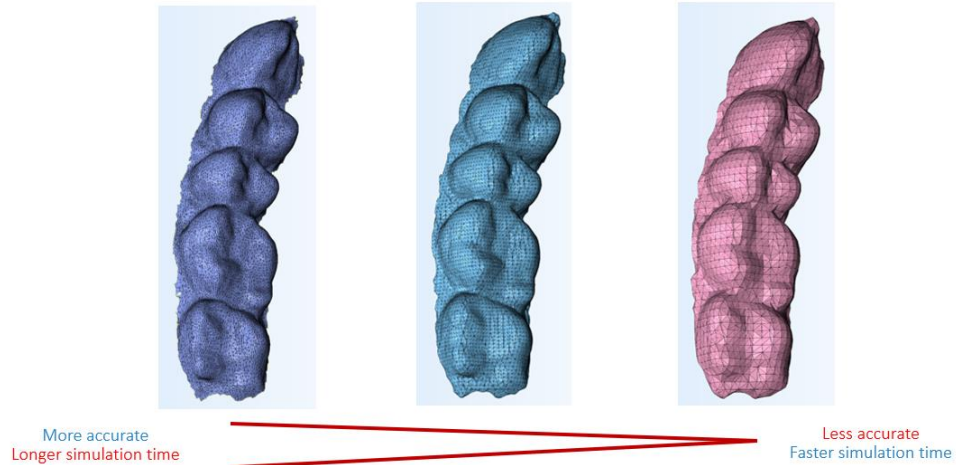


Figure 16. Reduction of Number of Mesh Elements. Diagram indicates tradeoff between high-resolution providing accuracy at the cost of a longer simulation time, and a lower resolution which can process faster.

The finalized meshed model is then converted from TET(4) into TET(10) elements to further improve accuracy in calculating the finite element model, and exported as an .INP model file ³⁴.

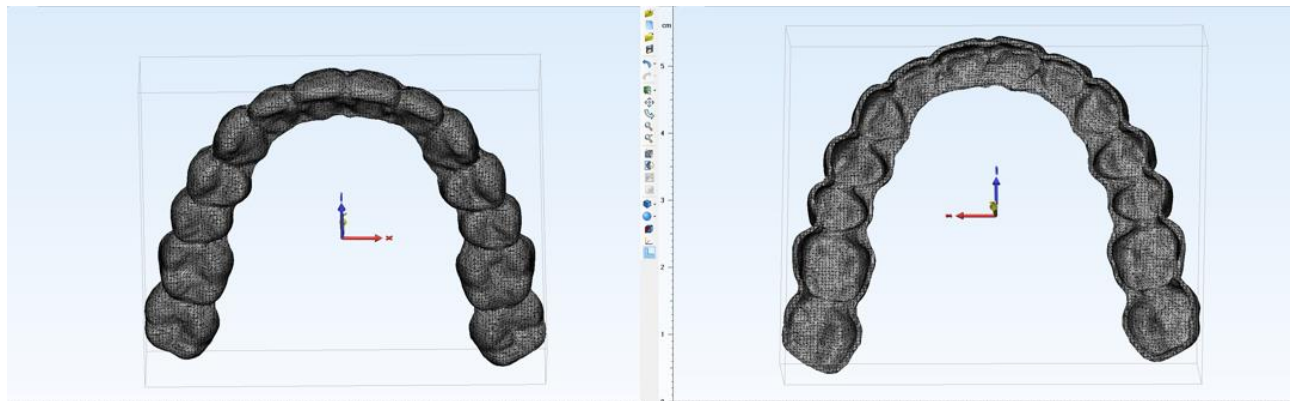


Figure 17. Refined Mesh after Smoothing and Noise removal.

Thicknesses of the digital aligner model will then be calibrated using actual measurements. Further, the specific material properties will be based on our measured Young’s modulus, with Poisson’s ratio for polyurethane derived from the literature.

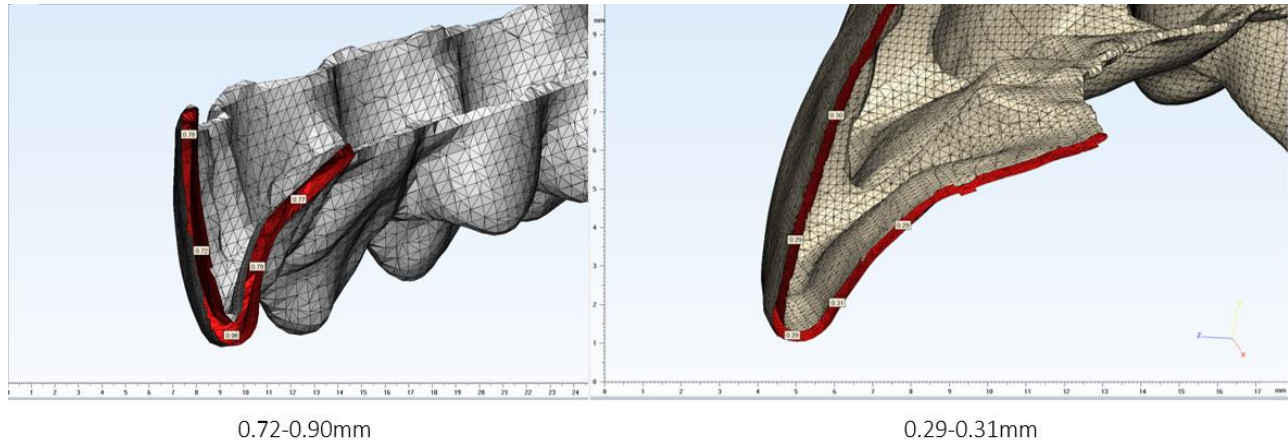


Figure 18. Calibration of Aligner Model Thickness. Using actual measurements for PETG at incisor tip (0.30mm), the model can be refined to meet these thickness dimensions.

After the import of refined mesh model of the aligner into ABAQUS (version 6.12, Dassault Systèmes, France), the volumetric elements and nodes will be isolated. The material will be assumed to be homogenous and isotropic. While for the enamel the a Young’s modulus of 15GPa and Poisson’s ratio of 0.33 will adequately represent the dentition³⁵, the Young’s modulus used here was 1361.32 MPa to represent 0.750mm Soaked PETG, with a Poisson’s ratio of 0.30 from the literature³⁶.

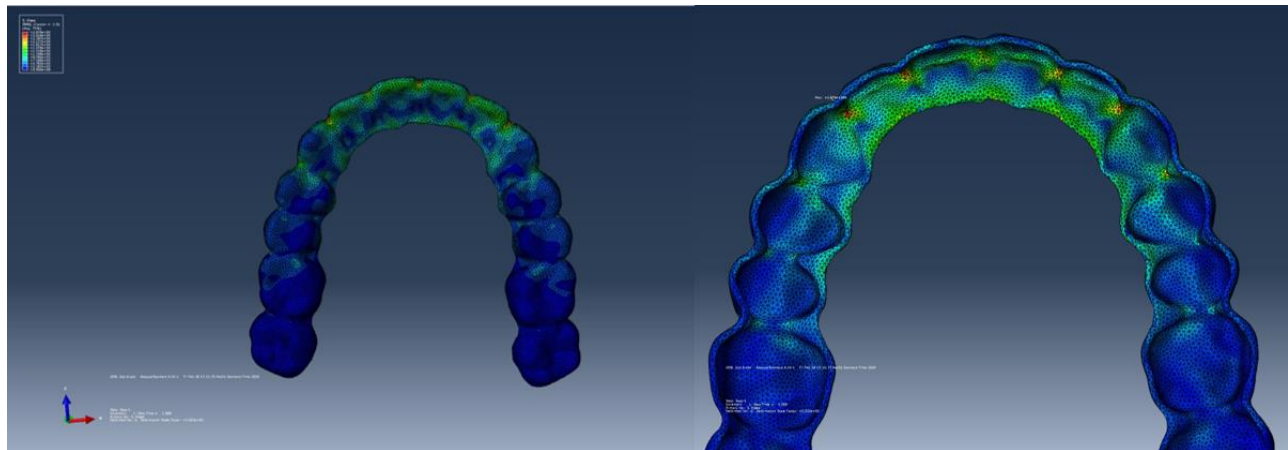


Figure 19. Finite Element Analysis Simulation on Clear Aligner Model.

Pictured above is the resulting FEA visualization. In this proof-of-concept scenario, one end of the aligner (patient’s upper right posterior) was fixed or encastered in all degrees of freedom (X, Y, and Z for pitch, roll, and yaw). At the same time, a light force of 8.89 Newtons (or approximately 2 pounds-force, or 101.97g)

was applied on the contralateral side. As expected, the force concentration is localized to the anterior region which corresponds to where the incisors are located.

DISCUSSION

The four mechanical testing methods used for this study have each shown certain strengths when it comes to comparing different materials, thicknesses, and whether it has been soaked and/or heat-treated or not. Starting off with microhardness, **Fig. 5** perhaps best summarizes the trends that would expect. Interestingly, heat formation differences can be detected for both TPU and PETG for the Dry state. Effects of soaking were minimal; only with PETG (both 0.625mm and 0.75mm) were any differences seen. This suggests that the PETG material could be more porous and have a higher absorption rate than does TPU. Effects of thickness on microhardness were essentially negligible, which seems intuitive since microhardness should be the same as it measures at the surface level. As for material choice, microhardness was shown to be able to distinguish between the two materials in the Raw-Dry, Raw-Soaked, and Aligned-Dry state. It seems that once the material was aligned and soaked, microhardness could no longer distinguish between TPU and PETG. Taken together, microhardness testing offers a wealth of insight especially for heat-formation and differing materials, but there are some limitations.

For crack or impact resistance testing, the overarching trend was that TPU consistently could withstand more impact than could PETG before reaching failure. This indicates that TPU has the ability to store more potential energy than PETG. In terms of thickness, no significant differences were observed for each material type. Except for 0.750mm TPU, the other groups show that the Aligned-Soaked group had the highest impact resistance. This is clinically significant as well since this is the state a patient's aligner resides in for the majority of its use.

With stress-strain testing using the Instron machine, there was a significant difference in modulus between PETG and TPU at 0.625mm in the Dry state. Within the TPU category, stress-strain testing detected significant differences if 1) the material had been soaked, and 2) if there was a thickness difference. Overall, stiffness of PETG was greater than that of TPU in the Dry state, but interestingly reversed for soaked, again suggesting PETG's absorption properties may be at play (as suspected for microhardness).

The last test, stress-relaxation, also sheds some clinically useful insight on the behavior of TPU versus PETG. From **Fig. 12A**, it is immediately apparent that Dry PETG 0.75mm has a significantly smaller amount of tensile stress change after 3 hours, both compared to its soaked counterparts along with the TPU group. While this could be due to small sampling or technical errors, it may also be explained by having potentially higher absorption properties than TPU. Overall, TPU at least at 0.75mm of thickness exhibits a slightly faster rate of relaxation (Fig. 12B) at 6.54 MPa/hr when soaked.

There are a few key clinical implications that we can take away from this study. The first is that almost all orthodontists at some point or another have received training on the basic mechanical properties of traditional wires in order to best utilize them during treatment. It follows then that the same will eventually hold true for clear aligners, especially now that numerous aligner formulations have gained a strong market presence. While this may not have been so crucial in the past when there were fewer brands to choose from, the current trend points towards a sizeable future selection of different aligner materials that will offer different degrees of performance and esthetic benefits. Thus, we have rationalized the importance and urgency to establish viable sets of mechanical testing parameters to objectively compare between different aligner types.

Specifically, in the current study, we have seen how TPU material compares in different conditions to PETG. The analogy that we can begin to draw is that TPU, with its ability to store more potential energy and faster rate of relaxation, behaves like a Nitinol wire which elicits a sustained, lighter orthodontic force. Conversely, PETG which presents with a higher Young's modulus can be likened to a stiffer stainless steel wire. Taken together, obtaining the appropriate material property values will provide clinicians with a better understanding and allow for more optimized treatment.

One early limitation we had faced was in preparing uniformly cut "dog bone" shaped aligner samples for Instron machine testing. Since a custom-fabricated and tooled punch and die would have been costly, a laser cutter was the next logical option. Unfortunately, our preliminary samples had shown a noticeable weakening when exposed to the laser cutter, as we speculate the generated heat had a negative effect on the

material. Thus, we had returned to the use of manual cutting with scissors. Although variation in dimensions would be inevitable with manual cutting, the Bluehill® Universal Test software testing parameters can be modified to specifically match the height, neck width, and thickness of individual specimens, which would help to reduce error.

Another drawback was due to the physical size limitations of some of the mechanical tests, certain testing modalities are only compatible with relatively large specimens. For example, the sample for crack resistance testing needs to be large enough to exceed the hole punch ring (1.63cm) to create an adequate punch. Fortunately, our workaround of thermoforming onto a raised platform strives to imitate the scenario and polymer deformation around a plaster dental cast. Likewise, this workaround was also necessary to create a large enough “dog bone” cut-out for stress-strain and stress-relaxation testing for the ‘aligned’ groups. To scale these methods to an actual thermoformed aligner would be impractical, and further the physical geometry of the aligner would confound our measurements.

In terms of future direction for this study, we would first strive to address the main short-comings of our stress-strain methodology as discussed above. The ideal candidate would be dynamic mechanical analysis, or DMA, which is a technique used to characterize the viscoelastic properties of polymeric materials. In a manner similar to the stress-strain test, a sinusoidal stress (σ) is applied to the sample and the strain, or displacement, of the material is measured³¹⁻³³. One key difference, however, is that the temperature of the sample can be varied, allowing for a complex modulus to be determined along with the glass transition temperature of the polymeric material. Additionally, since changes in composition of monomers and degree of cross-linking will have an effect in the results obtained from DMA, this means for testing will be appropriate in the context of this study. In fact, DMA has been incorporated in the material manufacturing industry as a means for quality control following the protocol guidelines set forth by American Society for Testing and Materials (ASTM) D7028³¹, which will also be used for this study using the Dynamic Mechanical Analyzer Q800 (TA Instruments, Delaware, USA). In the context of this study, it should allow for significantly smaller samples to be used and create a stress-strain, temperature-dependent profile in a fraction of the time.

Lastly, we are excited to bridge these mechanical testing results over to the clinical side with the help of our finite element model. The existence of a high-resolution FEA orthodontic aligner model is promising because of its versatility when it comes to biomechanical simulation, as we have established in our previous orthopaedic studies^{34,38,39}. While at its early stages, this model can be further improved through incorporation of either multi-layers or varying local material composition. Of course, stiffnesses and force load applications can be changed quickly and yield new insight without physical testing. And just as a contemporary orthodontic wire may have differential stiffness values in the anterior versus the posterior, we foresee the future of orthodontic aligners as having a custom ratio of both soft and stiff polymers to better optimize orthodontic tooth movements. Future studies could potentially develop this FEA model to ultimately create a custom aligner blend tailored to individual patients.

CONCLUSIONS

The selected mechanical testing methodologies have proven to be valuable in distinguishing between aligner material type, thickness, status of heat treatment, and soaking. With microhardness testing, both differences in heat formation and material selection could be detected, but it is best applied in the Dry state. For crack or impact resistance testing, the ability to distinguish between material types was not a difficult task, although it had issues with thickness differences and soaked samples. With stress-strain testing, distinguishing between materials was not an issue either in the Dry state at 0.625mm. Furthermore, it is promising since for TPU in all conditions it could distinguish for soaked and thickness status. Similarly, stress-strain results indicate a faster rate of relaxation for TPU overall. Lastly, a functional finite element model was successfully developed in the current study for future use in order to better model the physical behavior of a clear aligner given assigned material properties.

REFERENCES

1. Zheng, M., Liu, R., Ni, Z. & Yu, Z. Efficiency, effectiveness and treatment stability of clear aligners: A systematic review and meta-analysis. *Orthod Craniofac Res* **20**, 127-133 (2017).
2. Weir, T. Clear aligners in orthodontic treatment. *Aust Dent J* **62 Suppl 1**, 58-62 (2017).
3. Melkos, A.B. Advances in digital technology and orthodontics: a reference to the Invisalign method. *Med Sci Monit* **11**, PI39-42 (2005).
4. Lombardo, L. *et al.* Stress relaxation properties of four orthodontic aligner materials: A 24-hour in vitro study. *Angle Orthod* **87**, 11-18 (2017).
5. Alexandropoulos, A., Al Jabbari, Y.S., Zinelis, S. & Eliades, T. Chemical and mechanical characteristics of contemporary thermoplastic orthodontic materials. *Aust Orthod J* **31**, 165-70 (2015).
6. Lombardo, L. *et al.* Optical properties of orthodontic aligners--spectrophotometry analysis of three types before and after aging. *Prog Orthod* **16**, 41 (2015).
7. White, D.W., Julien, K.C., Jacob, H., Campbell, P.M. & Buschang, P.H. Discomfort associated with Invisalign and traditional brackets: A randomized, prospective trial. *Angle Orthod* **87**, 801-808 (2017).
8. Liu, C.L. *et al.* Colour stabilities of three types of orthodontic clear aligners exposed to staining agents. *Int J Oral Sci* **8**, 246-253 (2016).
9. Drake, C.T., McGorray, S.P., Dolce, C., Nair, M. & Wheeler, T.T. Orthodontic tooth movement with clear aligners. *ISRN Dent* **2012**, 657973 (2012).
10. Vardimon, A.D., Robbins, D. & Brosh, T. In-vivo von Mises strains during Invisalign treatment. *Am J Orthod Dentofacial Orthop* **138**, 399-409 (2010).
11. Gracco, A. *et al.* Short-term chemical and physical changes in invisalign appliances. *Aust Orthod J* **25**, 34-40 (2009).
12. Ahn, H.W., Ha, H.R., Lim, H.N. & Choi, S. Effects of aging procedures on the molecular, biochemical, morphological, and mechanical properties of vacuum-formed retainers. *J Mech Behav Biomed Mater* **51**, 356-66 (2015).

13. Hao-Fu Lee, B.W., Kang Ting. Preliminary Studies on Invisalign tray fabrication. *American Journal of Orthodontics and Dentofacial Orthopedics* **122**, 678 (2002).
14. Hendrikson, W.J., van Blitterswijk, C.A., Rouwkema, J. & Moroni, L. The Use of Finite Element Analyses to Design and Fabricate Three-Dimensional Scaffolds for Skeletal Tissue Engineering. *Front Bioeng Biotechnol* **5**, 30 (2017).
15. Gomez, J.P., Pena, F.M., Martinez, V., Giraldo, D.C. & Cardona, C.I. Initial force systems during bodily tooth movement with plastic aligners and composite attachments: A three-dimensional finite element analysis. *Angle Orthod* **85**, 454-60 (2015).
16. Barone, S., Paoli, A., Razionale, A.V. & Savignano, R. Computational design and engineering of polymeric orthodontic aligners. *Int J Numer Method Biomed Eng* (2016).
17. Dasy, H. *et al.* Effects of variable attachment shapes and aligner material on aligner retention. *Angle Orthod* (2015).
18. Azaripour, A. *et al.* Braces versus Invisalign(R): gingival parameters and patients' satisfaction during treatment: a cross-sectional study. *BMC Oral Health* **15**, 69 (2015).
19. Mc, L.J. An investigation into the physical properties, histopathology and clinical technique of the mouth temperature polymerizing resins. *Br Dent J* **89**, 215-26 (1950).
20. Pollmann, L. [Modulation of mouth temperature by thermal stimulation of the extremities]. *Dtsch Z Mund Kiefer Gesichtschir* **9**, 263-4 (1985).
21. Brebner, D.F., Kerslake, D.M. & Soper, D.G. Some effects of exposure to an environment of saturated air at mouth temperature. *J Physiol* **162**, 244-58 (1962).
22. Gungor, H., Gundogdu, M., Alkurt, M. & Yesil Duymus, Z. Effect of polymerization cycles on flexural strengths and microhardness of different denture base materials. *Dent Mater J* **36**, 168-173 (2017).
23. Kawaguchi, T., Lassila, L.V., Tokue, A., Takahashi, Y. & Vallittu, P.K. Influence of molecular weight of polymethyl(methacrylate) beads on the properties and structure of cross-linked denture base polymer. *J Mech Behav Biomed Mater* **4**, 1846-51 (2011).

24. Moshaverinia, A. *et al.* Measure of microhardness, fracture toughness and flexural strength of N-vinylcaprolactam (NVC)-containing glass-ionomer dental cements. *Dent Mater* **26**, 1137-43 (2010).
25. Ford, A.C. *et al.* Micromechanisms of fatigue crack growth in polycarbonate polyurethane: Time dependent and hydration effects. *J Mech Behav Biomed Mater* **79**, 324-331 (2018).
26. Zhang, Y. & Tanner, K.E. Impact behavior of hydroxyapatite reinforced polyethylene composites. *J Mater Sci Mater Med* **14**, 63-8 (2003).
27. Chandramohan, D. & Presin Kumar, A.J. Experimental data on the properties of natural fiber particle reinforced polymer composite material. *Data Brief* **13**, 460-468 (2017).
28. Krone, R., Havenstrite, K. & Shafi, B. Mechanical characterization of thin film, water-based polymer gels through simple tension testing of laminated bilayers. *J Mech Behav Biomed Mater* **27**, 1-9 (2013).
29. Zanelli, L., Todros, S., Carniel, E.L., Pavan, P.G. & Pavan, P.G. Mechanical properties variation and constitutive modelling of biomedical polymers after sterilization. *Acta Bioeng Biomech* **19**, 3-9 (2017).
30. Sweeney, J., Bonner, M. & Ward, I.M. Modelling of loading, stress relaxation and stress recovery in a shape memory polymer. *J Mech Behav Biomed Mater* **37**, 12-23 (2014).
31. Behin, P., Stoclet, G., Ruse, N.D. & Sadoun, M. Dynamic mechanical analysis of high pressure polymerized urethane dimethacrylate. *Dent Mater* **30**, 728-34 (2014).
32. Fernandez, J., Larranaga, A., Etxeberria, A. & Sarasua, J.R. Tensile behavior and dynamic mechanical analysis of novel poly(lactide/delta-valerolactone) statistical copolymers. *J Mech Behav Biomed Mater* **35**, 39-50 (2014).
33. Fadda, H.M. *et al.* The use of dynamic mechanical analysis (DMA) to evaluate plasticization of acrylic polymer films under simulated gastrointestinal conditions. *Eur J Pharm Biopharm* **76**, 493-7 (2010).
34. Lee, H. *et al.* Biomechanical effects of maxillary expansion on a patient with cleft palate: A finite element analysis. *Am J Orthod Dentofacial Orthop* **150**, 313-23 (2016).
35. Lee, J.H. *et al.* A novel method for the accurate evaluation of Poisson's ratio of soft polymer materials. *ScientificWorldJournal* **2013**, 930798 (2013).

36. Alberich-Bayarri, A. *et al.* Microcomputed tomography and microfinite element modeling for evaluating polymer scaffolds architecture and their mechanical properties. *J Biomed Mater Res B Appl Biomater* **91**, 191-202 (2009).
37. Vetter, T.R. Fundamentals of Research Data and Variables: The Devil Is in the Details. *Anesth Analg* **125**, 1375-1380 (2017).
38. James, A.W. *et al.* Vertebral Implantation of NELL-1 Enhances Bone Formation in an Osteoporotic Sheep Model. *Tissue Eng Part A* **22**, 840-9 (2016).
39. Chung, C.G. *et al.* Human perivascular stem cell-based bone graft substitute induces rat spinal fusion. *Stem Cells Transl Med* **3**, 1231-41 (2014).